

# Self-sustained lift and low friction via soft lubrication

Baudouin Saintyves,<sup>1</sup> Théo Jules,<sup>1,2</sup> Thomas Salez,<sup>1,3</sup> and L. Mahadevan<sup>4,\*</sup>

<sup>1</sup>*Paulson School of Engineering and Applied Sciences,  
Harvard University, Cambridge, MA 02138, USA*

<sup>2</sup>*Département de Physique, ENS, PSL Research University, 75005 Paris, France*

<sup>3</sup>*PCT Lab, UMR CNRS 7083 Gulliver, ESPCI ParisTech, PSL Research University, 75005 Paris, France*

<sup>4</sup>*Paulson School of Engineering and Applied Sciences, Department of Physics,  
Wyss Institute for Bioinspired Engineering and the Kavli Institute for Nanobio Science and Technology,  
Harvard University, Cambridge, MA 02138, USA*

(Dated: June 12, 2022)

Relative motion between soft wet solids arises in a number of applications in natural and artificial settings, and invariably couples elastic deformation and fluid flow. We explore this in a minimal setting by considering a fluid-immersed negatively-buoyant cylinder moving along a soft inclined wall. Our experiments show that there is a robust steady-state sliding regime of the cylinder with an effective friction that is significantly reduced relative to that of rigid fluid-lubricated contacts. A simple scaling approach that couples the cylinder-induced flow to substrate deformation allows us to explain the emergence of an elasto-hydrodynamic lift that underlies the self-sustained lubricated motion of the cylinder, consistent with recent theoretical predictions. Our results suggest an explanation for a range of effects such as reduced wear in animal joints and long-runout landslides, and can be couched as a design principle for low-friction interfaces.

Sliding motion between contacting solids arises in a range of phenomena that spans many length and time scales and includes landslides [1], aquaplaning of tires [2], industrial bearings [3], synovial and cartilaginous joints [5–9], cell motion in blood vessels and microfluidic devices [10, 11] and atomic-force and surface-force rheological apparatus [14]. In addition to friction and adhesion, invariably involve fluid lubrication and elastic deformation. To probe this class of phenomena in a minimal setting, we combine experiments and theory to show how a heavy fluid-lubricated particle can slide steadily along a soft incline with low effective friction. The origin of the low friction lies in a self-sustained lift that is due to the viscous-flow-induced fore-aft asymmetry of the deformation profile of the incline, and leads to an elasto-hydrodynamic analogue of Reynolds slider bearing [15]. This yields a scaling law for the steady velocity as a function of the fluid viscosity, the elastic modulus and thickness of the substrate, gravity, inclination angle, and the size of the particle, which we corroborate using experiments. Our study helps to explain a variety of elasto-hydrodynamic phenomena associated with low friction, while providing simple design principles for minimizing friction between soft moving interfaces.

Since the pioneering work of Reynolds [15], lubrication theory has been extensively studied, initially in the context of heavy industry [3], and more recently in the context of motion at soft material and biological interfaces [4]. In heavy load, high velocity settings, strongly confined induced viscous flows can generate high pressure and heat, with associated rheological piezoviscous, thermoviscous effects and nanometric substrate deformations [3]. In contrast, in light loading conditions

associated with steady sliding motions at soft wet interfaces, the coupling between elasticity and flow leads to long wavelength deformations that predict the emergence of lift and reduced friction [16–19]. Perhaps surprisingly, it is only recently that the problem of a free particle that can simultaneously sediment, slide or roll has been treated [20], with further predictions of a range of counterintuitive solutions such as enhanced sedimentation, bouncing, roll reversal and self-sustained long-runout sliding. Here we consider a minimal experimental setting to test these predictions, and focus in particular on the self-sustained elasto-hydrodynamic lift and the accompanying low effective friction associated with the motion of a heavy fluid-immersed cylinder sliding along a soft inclined wall.

Our setup, sketched in Fig. 1(a), consists of a glass plate (0.5 cm × 5 cm × 30 cm) mounted on a variable incline (angle  $\alpha$ ), coated with a thin layer of soft material (polyacrylamide-PAA or polydimethylsiloxane-PDMS with varying crosslinker and monomer concentrations, see SI) of thickness  $h$  and shear modulus  $G$ , immersed in a transparent aquarium (8 cm × 15 cm × 33 cm) filled with Rhodorsil silicone oil of density  $\rho_{\text{oil}} = 970 \text{ kg/m}^3$  and with varying viscosities  $\eta$ . Cylinders of radii  $R$ , made of different materials of density  $\rho$  (relative density  $\rho^* = \rho - \rho_{\text{oil}} > 0$ ), are allowed to slide down the incline after being launched manually, and their trajectory is followed using a simple wide-angle camera. To visualize the profile of the deformed coating, we embed fluorescent polyethylene particles at the elastic-oil interface, use a blue laser sheet to illuminate the interface from below, and focus a near-field macro-lens on the interface, as shown in Fig. 1(a); this allows us to see only the interface (Fig. 1(b), Movie M1). In a given experiment, we observe both spinning and sliding motions of the cylinder (Movie M2), so that the translation speed

\* lm@seas.harvard.edu

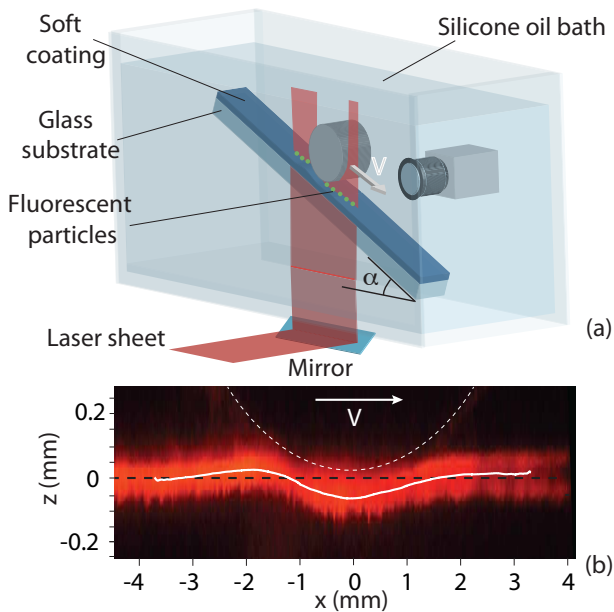


FIG. 1. **Experimental setup and laser profilometry.**

(a) A negatively-buoyant rigid cylinder immersed in a viscous bath slides down a tilted wall that is coated with a thin elastic layer. Fluorescent particles embedded in the latter allow for laser profilometry of the elastic layer-oil interface. (b) Side view of the substrate deformation (red) obtained with the laser sheet. The centre of the cylinder is located at  $x = 0$ . The white dashed line is a guide to the eye indicating the cylinder profile, the black dashed line corresponds to the unperturbed state of the substrate. The white solid line corresponds to the center of the fluorescent signal from the particles, obtained by using a transverse Gaussian fit, showing the asymmetric profile of the elastic layer-oil interface. The experimental parameters are  $G = 65$  kPa,  $h = 1.5$  mm,  $\eta = 1$  Pa.s,  $R = 12.7$  mm,  $\rho = 8510$  kg/m<sup>3</sup>,  $\alpha = 11^\circ$ .

is  $\dot{\theta}R + V$ , where  $\dot{\theta}$  is the angular velocity and  $V$  the sliding speed. For most experiments,  $V \gg R\dot{\theta}$  (except for motion on very soft gels, see SI) and thus we focus mainly on the sliding motion that is extracted via an image-processing algorithm.

For a base line, we first perform experiments with the cylinder moving down a rigid glass incline, and see stick-slip motion [21] rather than the theoretically predicted smooth motion of the cylinder [22, 23]; the dotted line in Fig. 2(a) highlights this intermittent low speed motion that is very sensitive to initial conditions. When the cylinder moves on a soft coating, there are a number of new effects. First, we observe that for certain combinations of cylinder size and density, the cylinder reverses its rolling direction (Movie M3), consistent with recent prediction [20]. Second, we also observe damped oscillations (Movie M4) when the cylinder is launched from a large height and it settles into its steady-state sliding motion, as predicted in [20]. Most strikingly, over a robust range of parameters, we observe a steady sliding of the cylinder accompanied by an asymmetrically

deformed elastic-oil interface (Movie M1), as shown in Fig. 1(b). This counter-intuitive observation suggests a mechanism for self-sustained lift at soft wet interfaces with implications for a range of phenomena that go beyond the simple instantiation here. It can be qualitatively understood by a simple modification of classical lubrication theory [15, 24]. For the case of rigid interfaces, the fore-aft symmetry of the gap implies that the pressure field is antisymmetric with a null normal resultant force. However, when the wall or cylinder is soft, this pressure asymmetry leads to an asymmetric elastic deformation [16–18, 20] that generates lift dynamically which is capable of sustaining the cylinder’s weight. Consistent with this, independent of initial conditions, over the entire range of tested substrate thicknesses and moduli, the cylinder achieves a robust sliding steady state (Fig. 2(a)) with a speed that is substantially higher than its speed when sliding along a rigid glass wall. The same behaviour is also qualitatively observed for elliptical cylinders (SI, Movie M5) – since these do not spin, we can clearly disregard rotation as the primary origin of self-sustained lift and reduced friction. Moving to quantify the role of the soft substrate, we note that the thicker (Fig. 2(a)) and the softer (Fig. 2(b)) the elastic layer, the higher the sliding speed, up to a certain point. In Fig. 2(b) we see that the sliding speed is a non-monotonic function of the modulus; it falls off for large moduli as expected, but also for small moduli owing to effects such as large substrate deformations (see Movie M6 for an example of an experiment with a very soft coating).

To minimally quantify the emergence of self-sustained lift and sliding motion of the cylinder at speed  $V$ , we limit ourselves to considerations of small strains in the elastic layer; as we will see, this suffices to explain most of our experiments. Assuming that the cylinder of radius  $R$  is separated from the undeformed substrate by a minimum gap  $\delta \ll R$ , the tangential size of the contact zone scales as  $l \sim \sqrt{R\delta}$ , so that  $\delta \ll l \ll R$ . This separation of scales allows us to invoke lubrication theory [24]. Then, the flow-induced pressure  $p$  scales as  $p \sim \eta V l / (\delta + \Delta h)^2$ , where  $\Delta h \sim h p / G \ll h$  is the normal elastic deformation of the soft layer [17, 25]. Together, this implies that the elasto-hydrodynamic pressure scales as  $\eta^2 V^2 R h / (G \delta^4)$  at leading order. Integrating this pressure over the contact length  $l$  leads to a positive elasto-hydrodynamic lift force per unit length that scales as  $\sim \eta^2 V^2 R^{3/2} h / (G \delta^{7/2})$  [17, 18].

At steady state,  $V = V_\infty$ , the elasto-hydrodynamic lift normal to the incline must balance the normal projection of the cylinder weight  $\sim \rho^* g R^2 \cos \alpha$ , while the tangential gravitational driving power  $\sim V_\infty \rho^* g R^2 \sin \alpha$  must balance the resisting viscous power  $\sim \eta (V_\infty / \delta)^2 l \delta$ . These relations yield the theoretical steady-state sliding speed:

$$V_\infty^{\text{th}} = A \frac{\rho^* g R^2 \sin \alpha}{\eta} \left( \frac{\rho^* g h \cos \alpha}{G} \right)^{1/5} \left( \frac{\sin \alpha}{\cos \alpha} \right)^{2/5}, \quad (1)$$

where  $A$  is a dimensionless constant. We note that  $V_\infty^{\text{th}}$  is the Stokes velocity  $\sim \rho^* g R^2 \sin \alpha / \eta$  of a parti-

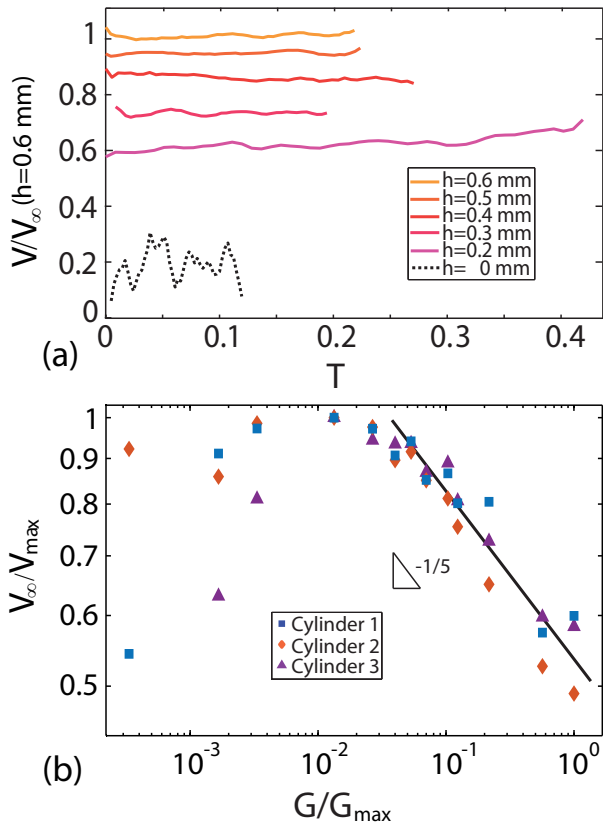


FIG. 2. **Sliding speed as a function of time and shear modulus of the substrate.** (a) Sliding speed  $V$  of an aluminium cylinder as a function of normalized time  $T = tV_\infty/d$ , for different thicknesses  $h$  of the soft coating. Here  $V_\infty$  is the time-averaged steady-state sliding speed,  $d$  the total length of the substrate, and  $t$  is the time. The vertical axis is normalized by  $V_\infty$  (for  $h = 0.6$  mm). The dotted line corresponds to the case of a bare glass substrate, while the solid lines are for coatings with an elastic layer of shear modulus  $G = 31$  kPa. The other experimental parameters are  $\rho = 2720$  kg/m<sup>3</sup>,  $R = 12.7$  mm,  $\eta = 1$  Pa.s, and  $\alpha = 11^\circ$ . (b) Time-averaged steady-state sliding speed for 3 different cylinders as a function of the shear modulus of the coating, with thickness  $h = 600$   $\mu$ m, oil bath viscosity  $\eta = 1$  Pa.s, and angle  $\alpha = 11^\circ$ . The vertical axis is normalized by the maximum steady-state sliding speed  $V_{\max}$  for the corresponding cylinder. The horizontal axis is normalized by the maximum of the tested moduli  $G_{\max} = 300$  kPa. The solid line has a slope of  $-1/5$  (Eq. (1)). The other parameters are as follows. Cylinder 1 (aluminium):  $\rho = 2720$  kg/m<sup>3</sup>,  $R = 12.7$  mm; cylinder 2 (glass):  $\rho = 2240$  kg/m<sup>3</sup>,  $R = 9.5$  mm; cylinder 3 (brass):  $\rho = 8510$  kg/m<sup>3</sup>,  $R = 6.35$  mm.

cle of size  $R$  in an infinite fluid, modified by the effect of elasto-hydrodynamics; indeed, the steady-state gap reads  $\delta_\infty \sim R(\rho^*gh \cos \alpha / G)^{2/5}(\sin \alpha / \cos \alpha)^{4/5}$  and allows us to rewrite the above scaling law in terms of the gap under more general loading conditions. A first check of Eq. (1) can be seen already in Fig. 2 showing evidence of

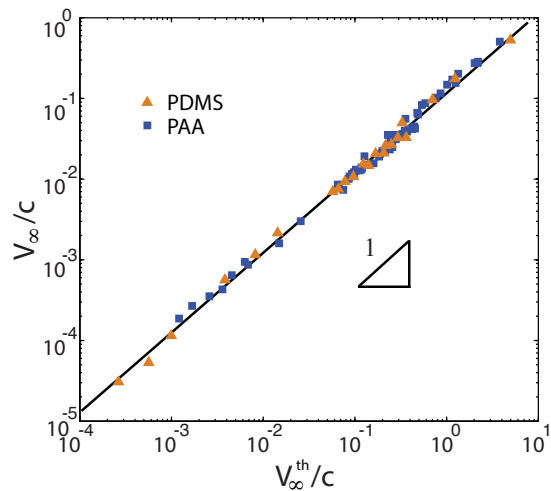


FIG. 3. **Master curve for steady sliding speed of an immersed cylinder on a soft substrate.** Time-averaged steady-state sliding speed  $V_\infty$  (Fig. 2) as a function of its theoretical prediction  $V_\infty^{\text{th}}$  (Eq. (1)). Both axes are scaled by the free fall speed  $c = \sqrt{2gR\rho^*/\rho}$ . The experiments were performed using either PDMS elastomers (triangles) or PAA hydrogels (squares). Both materials give overlapping results for a range of moduli. The solid line has unit slope.

the steady speed for a range of elastic layer thicknesses and moduli; furthermore, the speed is inversely proportional to  $G^{1/5}$  in the small deformation limit, i.e. for relatively stiff materials. To test Eq. (1) further, we used cylinders (all of width 12.7 mm) with radii  $R = 12.7$ , 9.5, and 6.35 mm, and densities  $\rho = 8510$ , 2720, and 2240 kg/m<sup>3</sup> corresponding to brass, aluminium and glass, moving in fluids with a range of viscosities  $\eta = 0.01$ , 0.35, 1, 30, and 100 Pa.s, along an incline with angle  $\alpha \in [10^\circ - 40^\circ]$ , that is coated with two different soft materials (PDMS, PAA) of modulus  $G \in [8 - 300]$  kPa (independently measured using a CP50 cone-plate geometry in an MCR 501 Anton Paar rheometer, see SI) and thickness  $h \in [100 \mu\text{m} - 2 \text{ mm}]$ . In Fig. 3, we see that the measured sliding speed is in excellent agreement with Eq. (1), over five decades in the scaled speed. Furthermore, the experimental prefactor  $A = 0.12 \pm 0.02$  in Eq. (1) is in good agreement with the theoretical prediction  $A \approx 0.2$  [20].

While Eq. (1) captures the small deformation regime associated with self-sustained lift and low friction, it cannot explain the decreasing of the sliding speed when the substrate is very soft, as shown in Fig. 2(b), because the ensuing large deformations require nonlinear developments of the present theory [18]. However, it is worth noting that steady state sliding is still observed in this regime and the sliding speed remains larger than in the case of a rigid substrate, suggesting that the lift force remains important even in this regime.

Our study of the motion of a fluid-immersed cylinder on a soft incline shows how self-sustained lift and low friction emerge dynamically due to the asymmetric elas-

tic deformation induced by the lubrication flow in the contact zone, in quantitative agreement with a recent theory [20]. These observations, when combined with substrate poroelasticity [17], may partly explain a variety of phenomena that couple flow and deformation at soft interfaces such as long run-out landslides [1] or low friction and wear of synovial joints [6]. Our study also points to a simple design principle for the reduction of friction and wear at soft interfaces, by tuning the elas-

tohydrodynamic interaction between soft particles using their shape and deformation properties. This might allow us to design fluid suspensions with controllable rheologies, including artificial analogs of normal and pathological blood [12, 13].

**Acknowledgments** We thank Shmuel Rubinstein for help with imaging, Jun Chung for discussions, and the MacArthur Foundation (LM) and the Harvard MRSEC DMR-1420570 for partial financial support.

- 
- [1] C. S. Campbell, *J. Geol.* 97, 653 (1989).
  - [2] F. Brochard-Wyart, *Compt. Rend. Phys.* 4(2), 207 (2003).
  - [3] B. J. Hamrock, ed., *Fundamentals of fluid film lubrication* (New York : McGraw-Hill, 1994).
  - [4] H. Zeng, ed., *Polymer adhesion, friction and lubrication* (Hoboken; Wiley, 2013).
  - [5] A. Maroudas, *Nature* 260, 808 (1976).
  - [6] G. W. Greene, X. Banquy, D. W. Lee, D. D. Lowrey, J. Yu, and J. N. Israelachvili, *Proceedings of the National Academy of Sciences* 108, 5255 (2011).
  - [7] A. J. Grodzinsky, H. Lipshitz, and M. J. Glimcher, *Nature* 275, 448 (1978).
  - [8] V. C. Mow and X. E. Guo, *Annu. Rev. Biomed. Eng.* 4, 175 (2002).
  - [9] V. C. Mow, M. H. Holmes, and W. M. Lai, *J. Biomech.* 17, 377 (1984).
  - [10] H. L. Goldsmith, *Fed Proc.* 30, 1578 (1971).
  - [11] S. Byun, S. Son, D. Amodi, N. Cermak, J. Shaw, J. H. Kang, V. C. Hecht, M. Winslow, T. Jacks, P. Mallick, et al., *PNAS (USA)* 110, 7580 (2013).
  - [12] J. M. Higgins, D. T. Eddington, S. N. Bhatia, and L. Mahadevan, *Proc. Natl. Acad. Sci.* 104, 2049620500 (2007).
  - [13] S. I. A. Cohen and L. Mahadevan, *Phys. Rev. Lett.* 110, 138104 (2013).
  - [14] R. Villey, E. Martinot, C. Cottin-Bizonne, M. Phaner-Goutorbe, L. Leger, F. Restagno, and E. Charlaix, *Phys. Rev. Lett.* 111, 101705 (2013).
  - [15] O. Reynolds, *Philos. Trans. R. Soc. Lond.* 177, 157 (1886).
  - [16] K. Sekimoto and L. Leibler, *Europhys. Lett.* 23, 113 (1993).
  - [17] J. M. Skotheim and L. Mahadevan, *Phys. Rev. Lett.* 92, 245509 (2004).
  - [18] J. M. Skotheim and L. Mahadevan, *Phys. Fluids* 17, 092101 (2005).
  - [19] J. H. Snoeijer, J. Eggers, and C. H. Venner, *Phys. Fluids* 25, 101705 (2013).
  - [20] T. Salez and L. Mahadevan, *J. Fluid Mech.* 779, 181 (2015).
  - [21] F. P. Bowden and D. Tabor, *Friction: an introduction to tribology* (Garden City, N.Y.: Anchor Press, 1973).
  - [22] H. Brenner, *J. Fluid Mech.* 12, 35 (1962).
  - [23] D. J. Jeffrey and Y. Onishi, *Quart. J. Mech. App. Math.* 34, 129 (1981).
  - [24] G. K. Batchelor, *An Introduction to Fluid Dynamics* (Cambridge University Press, Cambridge, England, 1967).
  - [25] K. L. Johnson, *Contact Mechanics* (Cambridge University Press, Cambridge, England, 1985).